

## SI Appendix

### Supplemental Materials and Methods

#### DNA

The cDNA fragments encoding mouse Fhod3 of cardiac muscle isoform (Fhod3CM) of 1,586 amino acids that contains all the 28 exons (previously designated as Fhod3-T(D/E)<sub>5</sub>XE(+)) in (1)) (Fig. 1E) and mouse Fhod3CM-IA carrying the I1127A substitution (2) were prepared as previously described (1, 2). The cDNA fragment for mouse Fhod3CM-S that contains all exons except exons 11 and 12 (Fig. 1E) was constructed from cDNAs for Fhod3CM and Fhos2S of 1,427 amino acids that lacks exons 11, 12, and 25 (3). The cDNA for the N-terminus (amino acids 1–569) of Fhod3CM and that of Fhod3CM-S (Fig. 2D) were constructed by PCR using the cDNAs encoding mouse Fhod3CM and Fhod3CM-S, respectively. The cDNA for mouse cMyBP-C (NM\_008653) was obtained by RT-PCR using RNAs prepared from the mouse heart. The DNA fragments encoding various lengths of cMyBP-C were prepared by PCR using the full-length cDNA. Mutations leading to the indicated amino acid substitutions were introduced by PCR-mediated site-directed mutagenesis. The cDNAs were ligated to pGEX-6P (GE Healthcare) or pEF-BOS for expression as GST fusion protein in *Escherichia coli* or for expression in HEK-293F cells as an N-terminally FLAG-tagged protein, respectively. All the constructs were sequenced for confirmation of their identities.

#### Mice

Transgenic mice expressing wild-type Fhod3CM (*Fhod3*<sup>Tg( $\alpha$ -MHC-Fhod3CM)</sup>) under the control of the  $\alpha$ -myosin heavy chain ( $\alpha$ -MHC) promoter, a generous gift from Dr. Jeffery Robbins

(Cincinnati Children's Hospital Medical Center) (4), were generated on a C57BL/6 background. Four different founder mice expressing wild-type Fhod3CM were obtained, but only three mice survived to reproductive age (#1, #8, and #11); expression level of exogenous Fhod3 in the transgenic mice was twenty-fold more than that of endogenous Fhod3 (Fig. S2). Data obtained from the line #1 were shown in the present study, while other lines showed essentially the same results. Transgenic mice expressing a mutant Fhod3CM-IA (*Fhod3*<sup>Tg(α-MHC-Fhod3CM-IA)</sup>) or a short variant Fhod3CM-S (*Fhod3*<sup>Tg(α-MHC-Fhod3CM-S)</sup>) under the control of α-MHC promoter were also generated on a C57BL/6 background. Only one transgenic line expressing Fhod3CM-IA or Fhod3CM-S was obtained from over 200 injections. Expression level of exogenous Fhod3CM-IA in the transgenic mice was five-fold more than that of endogenous Fhod3 (Fig. S2). Protein expression level of exogenous Fhod3CM-S was substantially lower than that of endogenous Fhod3 but the presence of mRNA was confirmed by RT-PCR (Fig. S9). The transgenic mice used in the present study (*Fhod3*<sup>Tg(α-MHC-Fhod3CM)</sup>, *Fhod3*<sup>Tg(α-MHC-Fhod3CM-S)</sup>, and *Fhod3*<sup>Tg(α-MHC-Fhod3CM-IA)</sup>) differ from our previous transgenic mice (*Fhod3*<sup>Tg(α-MHC-Fhod3)</sup> and *Fhod3*<sup>Tg(α-MHC-Fhod3-IA)</sup>) (1, 5) with respect to the presence of the T(D/E)<sub>5</sub>XE region encoded by exon 25 (see Fig. 1E).

Mice carrying the *Mybpc3*<sup>tm1a(EUCOMM)Hmgu</sup> allele (B6Dnk;B6N-Mybpc3<sup>tm1a(EUCOMM)Hmgu</sup>/H) (EMMA ID EM:04690) were obtained from the European Mouse Mutant Archive, and subsequently crossed with mice expressing flipase (6) to obtain animals heterozygous for the floxed *Mybpc3* allele (*Mybpc3*<sup>lox/+</sup>) (Fig. S10). cMyBP-C knockout mice were generated by crossing the *Mybpc3*<sup>lox/+</sup> with *Meox2*<sup>Cre/+</sup> mice (7) (The Jackson laboratory), which express Cre recombinase in the embryo before implantation, and the offspring were further crossed with C57BL/6 to generate *Mybpc3*<sup>+/-</sup> mice without the Cre transgene. Deletion of exons 3, 4, and 5 of *Mybpc3* gene by this strategy is expected to result in complete depletion of cMyBP-C protein, since the truncated

cMyBP-C peptides was not found in the previous reports (8–10). *Mybp3*<sup>-/-</sup> mice survived to adulthood and were fertile, although they showed cardiomyopathic changes as previously reported (8, 11, 12).

All the experimental protocol was approved by the Animal Care and Use Committee of Kyushu University (Permit Number: A26-102) and the Animal Care and Use Committee of University of Miyazaki (Permit Number: 2014-526-3). All mice were housed and maintained in a specific pathogen-free animal facility at Kyushu University or at University of Miyazaki, and all efforts were made to minimize the number of animals used and their suffering. All experiments were performed in strict accordance with the guidelines for Proper Conduct of Animal Experiments (Science Council of Japan).

### **Neonatal Rat Cardiomyocytes**

Primary cultures of neonatal rat cardiomyocytes were prepared as described previously (13). Transfection of cardiomyocytes with the adenoviruses encoding HA-tagged mouse Fhod3 and their mutants were performed as described previously (13).

### **Antibodies**

Rabbit anti-Fhod3 polyclonal antibodies were raised against three different regions of Fhod3, namely, anti-Fhod3-(650–802), anti-Fhod3-(873–974), and anti-Fhod3-C20, followed by affinity purification, as previously described (3). Anti- $\alpha$ -actinin monoclonal antibody (EA-53) was purchased from Sigma-Aldrich; anti-MHC monoclonal antibody (MF20) from Developmental Studies Hybridoma Bank (Iowa City, IA); anti-MHC monoclonal antibody (3-48) from Abcam; anti-cMyBP-C monoclonal antibody (G-7) from Santa Cruz; anti- $\alpha$ -tubulin monoclonal antibody (10G10) from WAKO; anti-glyceraldehyde-3-phosphate dehydrogenase (GAPDH) (6C5) from Chemicon;

anti-FLAG peptide monoclonal antibody (M2) from Sigma-Aldrich; anti-HA peptide monoclonal antibody (16B12) from Covance. Anti-cMyBP-C polyclonal antibodies (M-190) were purchased from Santa Cruz. Alexa Fluor 488-conjugated F(ab')<sub>2</sub> fragment of anti-mouse IgG and Alexa Fluor 555-conjugated F(ab')<sub>2</sub> fragment of anti-rabbit IgG were purchased from Cell Signaling Technology. Alexa Fluor 680-conjugated goat anti-mouse IgG was from Thermo Fisher Scientific.

### **Protein Identification by LC–MS/MS Analysis**

To obtain Fhod3-binding proteins, the immunoprecipitated proteins with anti-Fhod3 antibodies were identified by mass spectrometry according to the method of Matsuzaki et al (14). Briefly, the immunoprecipitated proteins were separated by SDS/PAGE and stained with silver. The stained gel was sliced into 10 equal pieces per lane, and the proteins therein were subjected to in-gel digestion with trypsin. The resulting peptides were dried, dissolved in a mixture of 0.1% trifluoroacetic acid and 2% acetonitrile, and then applied to a nanoflow LC system (Paradigm MS4; Michrom BioResources, Auburn, CA) equipped with an L-column (C18, 0.15 × 50 mm, particle size of 3 μm; CERI, Tokyo, Japan). The peptides were fractionated with a linear gradient of solvent A (2% acetonitrile and 0.1% formic acid in water) and solvent B (90% acetonitrile and 0.1% formic acid in water), with 0–45% solvent B over 20 min, 45–95% over 5 min, and 95–5% over 1 min at a flow rate of 1 μl/min. Eluted peptides were sprayed directly into a Finnigan LTQ mass spectrometer (Thermo Fisher Scientific, San Jose, CA). MS and MS/MS spectra were obtained automatically in a data-dependent scan mode with a dynamic exclusion option. All MS/MS spectra were compared with protein sequences in the International Protein Index (IPI; European Bioinformatics Institute, Hinxton, United Kingdom) with the use of the MASCOT algorithm. Trypsin was selected as the enzyme used, the allowed number of missed cleavages was set at

one, and carbamidomethylation of cysteine was selected as a fixed modification. Oxidized methionine and NH<sub>2</sub>-terminal pyroglutamate were searched as variable modifications. Tolerance of MS/MS ions was 0.8 Da. Assigned high-scoring peptide sequences (MASCOT score of > 45) were considered for correct identification.

### **Immunoprecipitation**

Immunoprecipitation analysis was performed as previously described (2) with minor modifications. Briefly, the hearts were lysed at 4°C with a lysis buffer (10% glycerol, 135 mM NaCl, 5 mM EDTA, and 20 mM Hepes, pH 7.4) containing 0.1% Triton X-100. The lysates were precipitated with the anti-Fhod3 or anti-cMyBP-C antibody in the presence of protein G-Sepharose or protein G-magnetic beads. After washing three times with the lysis buffer containing 0.1% Triton X-100, the precipitants were applied to SDS-PAGE and transferred to a polyvinylidene difluoride membrane (Millipore). The membrane was probed with the anti-Fhod3 or anti-cMyBP-C antibodies, followed by development using ECL-prime (GE Healthcare) for visualization of the antibodies.

### **An *in vitro* Pull-down Binding Assay**

GST-tagged proteins were expressed in *Escherichia coli* strain BL21 and purified by glutathione-Sepharose-4B (GE Healthcare). FLAG-tagged Fhod3 proteins were expressed in HEK-293F cells and purified by an anti-FLAG antibody (M2)-conjugated agarose (Sigma). Pull-down binding assays were performed as previously described (15), with minor modifications. Briefly, GST-cMyBP-C was mixed with the lysate of HEK-293F cells expressing FLAG-tagged Fhod3 or purified FLAG-tagged Fhod3 and incubated for 60 min at 4°C in 1 ml of a lysis buffer (10% glycerol, 135 mM NaCl, 5 mM EDTA, 0.1% Triton X-100, and 20 mM Hepes, pH 7.4) containing Protease Inhibitor Cocktail (Sigma-Aldrich). Proteins

were pulled down with glutathione-Sepharose 4B beads, washed three times with the lysis buffer, subjected to SDS-PAGE, and stained with *Coomassie Brilliant Blue* (CBB) or analyzed by immunoblot with the indicated antibodies.

For the competition assay (Fig. 3E), GST–cMyBP-C-C0C2 bound to MagneGST glutathione particles (Promega) was incubated with the lysate of HEK-293F cells expressing FLAG-tagged Fhod3CM(N) (final concentration of 2.0  $\mu$ M) in the presence of various concentration of heavy meromyosin (purified from rabbit muscle; Cytoskeleton) for 60 min at 4°C in a lysis buffer. Proteins were collected with glutathione particles, washed three times, subjected to SDS-PAGE, and analyzed by immunoblot.

In the case of quantitative analysis (Fig. 3F and G), GST–cMyBP-C-C0 or GST alone immobilized to MagneGST glutathione particles was incubated with various concentrations of the lysate of HEK-293F cells expressing FLAG-tagged Fhod3CM(N) in 500  $\mu$ l of a buffer (1% glycerol, 104 mM NaCl, 0.5 mM EDTA, 0.1% Triton X-100, and 20 mM Hepes, pH 7.4). Bound proteins were collected with glutathione particles without washing, subjected to SDS-PAGE, and analyzed by immunoblot with the anti-FLAG antibodies followed by fluorescence measurement using the image analyzer LAS-3000 (Fuji Photo Film).

### **Immunoblot Analysis**

Immunoblot analysis was performed as previously described (2). Briefly, the hearts of mice were snap-frozen, crushed using SK-Mill (SK-100, FUNAKOSHI), and dissolved in a buffer composed of 9 M Urea, 2% SDS, 2% Triton X-100, 1% dithiothreitol, and 10 mM Tris-HCl, pH 6.8, containing Protease Inhibitor Cocktail (Sigma-Aldrich). The lysates were applied to SDS-PAGE and was transferred to a polyvinylidene difluoride membrane (Millipore). The membrane was probed with the antibody, followed by development using ECL-prime (GE

Healthcare) for visualization of the antibodies. For the quantitative analysis, membrane was probed with Alexa Fluor 680-conjugated anti-mouse IgG and images are acquired using LAS-3000. Positions for marker proteins are indicated in kDa.

### **Immunofluorescence Staining of Cardiac Sections**

Immunofluorescence staining was performed according to the previously described method (2) with minor modifications. Briefly, mice were deeply anesthetized with an intraperitoneal injection of pentobarbital (50 mg/kg/body weight) and sevoflurane inhalation. After exposure of the heart, PEM buffer (1 mM EGTA, 1 mM MgCl<sub>2</sub>, and 100 mM PIPES, pH 6.9) containing 100 mM 2,3-butanedione monoxime (BDM) was administered from the left ventricular apex, followed by the administration of 3.7% formaldehyde in the PEM buffer. The fixed hearts were removed from the deceased mice, cut into small pieces, and immersed for 90 min at 4°C in the same fixative. The fixed hearts were washed in PBS, subjected to osmotic dehydration overnight at 4°C in 30% sucrose, and embedded in OCT compound (Sakura Finetek). The blocks were frozen and cut into 5 µm sections using a cryostat HM550 (Thermo Scientific) or CM3050S (Leica Biosystems). Sections were then washed with PBS containing 0.1% Triton X-100, and blocked with a blocking buffer (Blocking One Histo; Nacalai tesque) for 15 min at room temperature. Sections were labeled overnight at 4°C with primary antibodies diluted in a dilution buffer (PBS containing 3% bovine serum albumin, 2% goat serum, and 0.1% Triton X-100), and then labeled for 2 h at room temperature with a fluorescein-conjugated secondary antibody mixture in the same buffer. For Fhod3 immunofluorescence staining, anti-Fhod3-(650–802) antibody were used. Actin filaments were stained with Alexa Fluor 488 phalloidin (Invitrogen). Nuclei were stained with Hoechst 33342 (Invitrogen). Membranes were stained with FITC-conjugated wheat germ agglutinin (J-Oil Mills). Images were taken with LSM700 or LSM780 confocal scanning laser

microscope (Carl Zeiss MicroImaging).

### **Quantitative Analysis of Fhod3 Distribution Pattern**

Fhod3 distribution pattern in the sarcomere was examined using line scan profiles of fluorescence intensities for the Fhod3 immunostaining of the heart tissues. The full-width at half-maximum was measured from fitting curves for Fhod3 intensity profiles using data analysis software (ORIGIN; OriginLab). Measurements had to have a Gaussian fit of  $R^2 > 0.9$ .

### **Histological Analysis**

Histological analysis was performed as previously described (2). Briefly, mice were sacrificed via cervical dislocation, and the whole heart was harvested. The harvested organs were fixed by immersion in a solution containing 3.7% formaldehyde in phosphate buffer saline (PBS; 137 mM NaCl, 2.68 mM KCl, 8.1 mM Na<sub>2</sub>HPO<sub>4</sub>, and 1.47 mM KH<sub>2</sub>PO<sub>4</sub>, pH 7.4). The obtained organs were dehydrated in ethanol, embedded in paraffin, sectioned, and stained with hematoxylin and eosin staining. Images were taken with BZ-9000 microscope (Keyence).

### **Quantification of mRNA Levels by Real-time PCR**

Total RNAs were extracted from the left ventricular tissue using TRIzol reagent (Invitrogen). Complementary DNAs were synthesized using SuperScript First-Strand (Invitrogen). Quantitative real-time PCR were performed using SYBR Premix Ex Ta II (TaKaRa Bio) on the LightCycler 480 system (Roch Diagnostics GmbH) with the following primer pairs for atrial natriuretic factor (ANF), B-type natriuretic peptide (BNP),  $\beta$ -myosin heavy chain ( $\beta$ -MHC), and glyceraldehyde-3-phosphate dehydrogenase (GAPDH) as an internal standard:



ANF, forward 5'-TTCCTCGTCTTGGCCTTTTG-3' and reverse  
3'-CCTCATCTTCTACCGGCATC-5'; BNP, forward  
5'-GTCAGTCGTTTGGGCTGTAAC-3' and reverse  
3'-AGACCCAGGCAGAGTCAGAA-5';  $\beta$ -MHC, forward  
5'-CGCATCAAGGAGCTCACC-3' and reverse 3'-ACCTTGGAGACCTCTTTTTGC-5';  
and GAPDH, forward 5'-GGAAGCCCATCACCATCTTCCA-3' and reverse  
3'-CCTTCTCCATGGTGGTGAAGAC-5'.

### **Transmission Electron Microscopic Analysis**

Transmission electron microscopy of thin sections was performed according to the previously described method (5) with minor modifications. Briefly, mice were deeply anesthetized with an intraperitoneal injection of pentobarbital and sevoflurane inhalation. After exposure of the heart, the PEM buffer containing 100 mM BDM was administered from the left ventricular apex, followed by the administration of the fix solution (2.0 % paraformaldehyde, 2.5% glutaraldehyde and 0.1 M sodium cacodylate, pH 7.4) for 2 h. The fixed tissue was rinsed in PBS, postfixed in 1% osmium tetroxide, dehydrated in ethanol and propylene oxide, and embedded in epoxy resin. Thin sections containing the heart were stained with uranyl acetate and lead citrate, and then examined with HT7700 (Hitachi).

### **Echocardiography**

Serial echocardiographic examinations were performed non-invasively using a 15-MHz high frequency linear transducer connected to SONOS 5500 system (Philips). Under anesthesia with an intraperitoneal injection of a combination anesthetic (0.15 mg/kg of medetomidine, 2.0 mg/kg of midazolam, and 2.5 mg/kg of butorphanol), two-dimensional targeted M-mode images were obtained from the long-axis view. Echocardiographic images were analyzed by

the analysis software of SONOS 5500. Left ventricular diastolic and systolic diameters (LVDD and LVDs), interventricular septum thickness (IVS) were measured following the guidelines of American Society of Echocardiography. The left ventricular ejection fraction (LVEF) was calculated according to the Teichholz method.

### **Statistics**

All data were expressed as mean  $\pm$  SEM. Two groups were compared by paired or unpaired Student's *t* test. Multiple groups were compared by analysis of variance followed by post-hoc Tukey test. A *P* value of  $<0.05$  was considered to be statistically significant. GraphPad Prism 5.0 (GraphPad Software Inc., San Diego, CA) was used for all statistical analysis.

## Supplemental References

1. Kan-o M, et al. (2012) Expression and subcellular localization of mammalian formin Fhod3 in the embryonic and adult heart. *PLoS One* 7(4):e34765.
2. Fujimoto N, et al. (2016) Transgenic expression of the formin protein Fhod3 selectively in the embryonic heart: role of actin-binding activity of Fhod3 and its sarcomeric localization during myofibrillogenesis. *PLoS One* 11(2):e0148472.
3. Kanaya H, et al. (2005) Fhos2, a novel formin-related actin-organizing protein, probably associates with the nestin intermediate filament. *Genes Cells* 10(7):665–678.
4. Gulick J, Subramaniam A, Neumann J, Robbins J (1991) Isolation and characterization of the mouse cardiac myosin heavy chain genes. *J Biol Chem* 266(14):9180–9185.
5. Kan-o M, et al. (2012) Mammalian formin Fhod3 plays an essential role in cardiogenesis by organizing myofibrillogenesis. *Biol Open* 1(9):889–896.
6. Kanki H, Suzuki H, Itohara S (2006) High-efficiency CAG-FLPe deleter mice in C57BL/6J background. *Exp Anim* 55(2):137–141.
7. Tallquist MD, Soriano P (2000) Epiblast-restricted Cre expression in MORE mice: a tool to distinguish embryonic vs. extra-embryonic gene function. *Genesis* 26(2):113–5.
8. Harris SP, et al. (2002) Hypertrophic cardiomyopathy in cardiac myosin binding protein-C knockout mice. *Circ Res* 90(5):594–601.
9. Chen PP, Patel JR, Powers PA, Fitzsimons DP, Moss RL (2012) Dissociation of Structural and Functional Phenotypes in Cardiac Myosin-Binding Protein C Conditional Knockout Mice. *Circulation* 126(10):1194–1205.
10. Nixon BR, et al. (2017) Alterations in sarcomere function modify the hyperplastic to hypertrophic transition phase of mammalian cardiomyocyte development. *JCI insight* 2(4):e90656.

11. McConnell BK, et al. (1999) Dilated cardiomyopathy in homozygous myosin-binding protein-C mutant mice. *J Clin Invest* 104(9):1235–44.
12. Carrier L, et al. (2004) Asymmetric septal hypertrophy in heterozygous cMyBP-C null mice. *Cardiovasc Res* 63(2):293–304.
13. Taniguchi K, et al. (2009) Mammalian formin Fhod3 regulates actin assembly and sarcomere organization in striated muscles. *J Biol Chem* 284(43):29873–29881.
14. Matsuzaki F, Shirane M, Matsumoto M, Nakayama KI (2011) Protrudin serves as an adaptor molecule that connects KIF5 and its cargoes in vesicular transport during process formation. *Mol Biol Cell* 22(23):4602–20.
15. Takeya R, Taniguchi K, Narumiya S, Sumimoto H (2008) The mammalian formin FHOD1 is activated through phosphorylation by ROCK and mediates thrombin-induced stress fibre formation in endothelial cells. *EMBO J* 27(4):618–628.

**Figure S1 (Matsuyama *et al.*)**

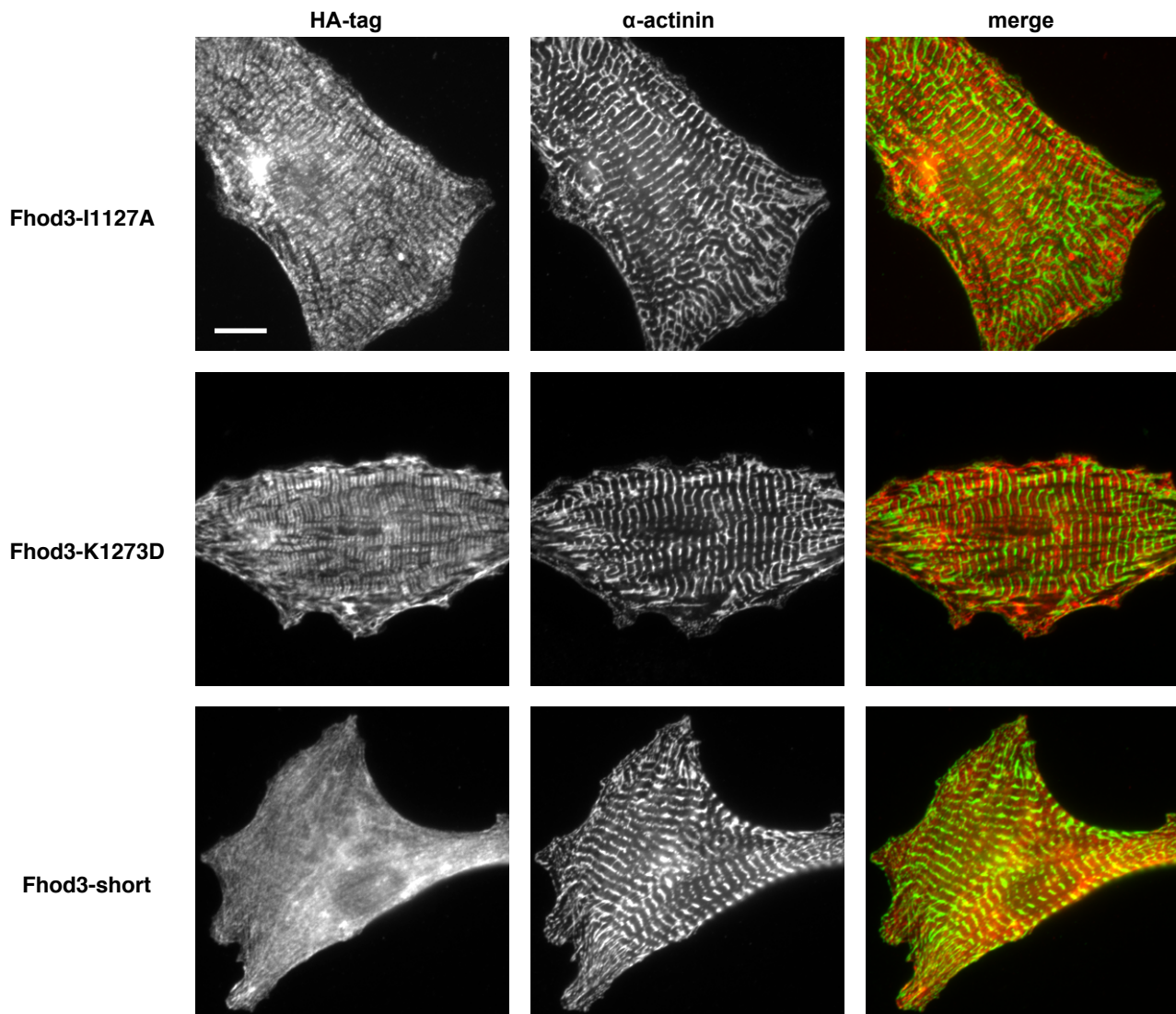


**Figure S1. Localization of mutant Fhod3 proteins in the cardiac sarcomere.** Neonatal rat cardiomyocytes transfected with the adenovirus encoding HA-tagged Fhod3 mutants were fixed and stained with the antibodies against anti-HA (red) and α-actinin (green). Scale bar, 10 μm.

## Figure S2 (Matsuyama *et al.*)

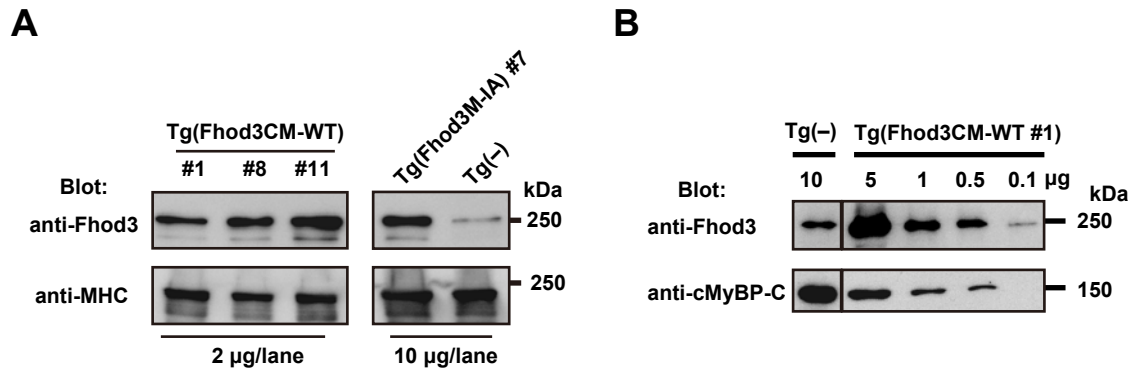


**Figure S2. Cardiac expression of Fhod3 in the transgenic mice expressing Fhod3CM-WT and Fhod3CM-IA.** (A) Fhod3 expression levels for independent transgenic lines. The indicated amount of cardiac lysates from transgenic mice (Tg(Fhod3CM-WT) or Tg(Fhod3CM-IA)) (see Fig. 1E) were analyzed by immunoblot with the anti-Fhod3-(C-20) and anti-MHC (3-48) antibodies. (B) Comparison of Fhod3 expression levels between Tg(Fhod3CM-WT) line #1 and non-transgenic control mice. The indicated amount of cardiac lysates from transgenic mice (Tg(Fhod3CM-WT) line #1) and Tg(-) mice were analyzed by immunoblot with the anti-Fhod3-(C-20) and anti-cMyBP-C antibodies. Experimental data obtained using the line #1 were shown in the present study.

Figure S3 (Matsuyama *et al.*)

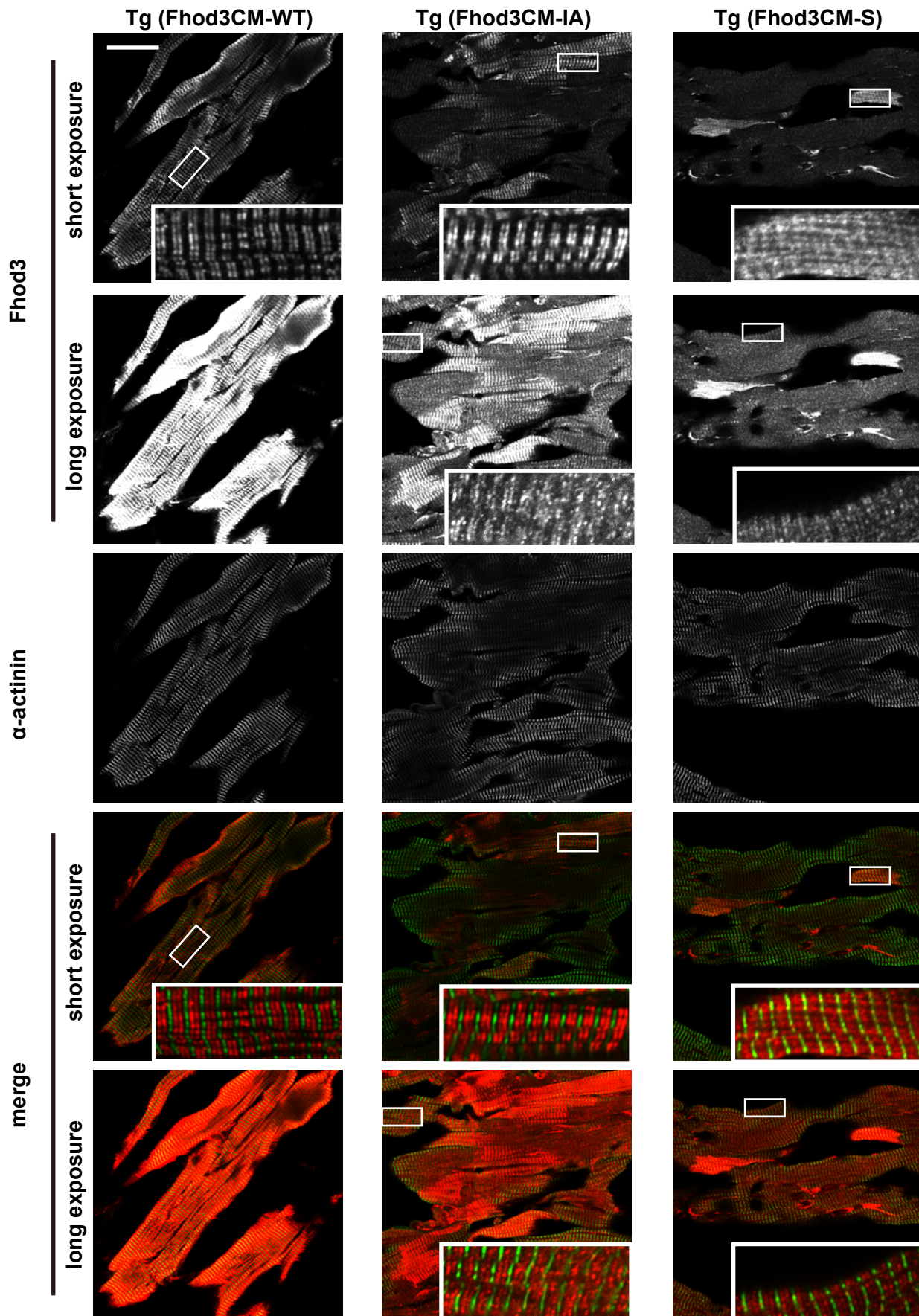


**Figure S3. Transgenic expression of Fhod3 variants in the heart.** Sections of adult hearts from transgenic mice expressing Fhod3CM-WT (left panels) (see Fig. 1E), Fhod3CM-IA (middle panels), and Fhod3CM-S (right panels) were subjected to immunofluorescent double staining for Fhod3 (anti-Fhod3-(650-802); red) and  $\alpha$ -actinin (green). Two different exposures for Fhod3 are shown in order to visualize the expression patterns of endogenous and exogenous Fhod3 proteins. Scale bar, 50  $\mu$ m.



**Figure S4 (Matsuyama *et al.*)**

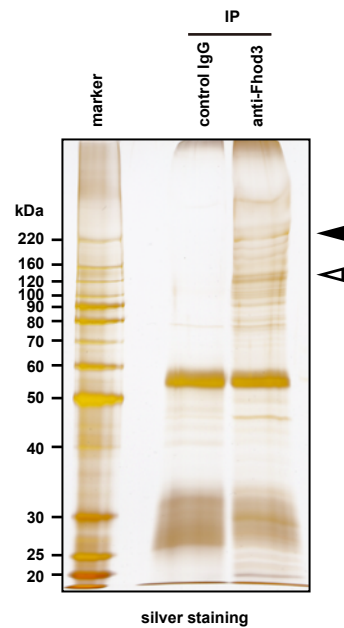


**Figure S4. Identification of Fhod3-binding proteins.** Proteins in a cardiac lysate from transgenic mice expressing Fhod3CM-WT were immunoprecipitated with the anti-Fhod3-C20 antibodies or control IgG, and fractionated by SDS-PAGE and stained with silver. The black and white arrowheads indicate the positions of Fhod3 and cMyBP-C, respectively. The stained gel was sliced and the proteins therein were subjected to mass spectrometric analysis (see Materials and Methods).



**Figure S5 (Matsuyama *et al.*)**

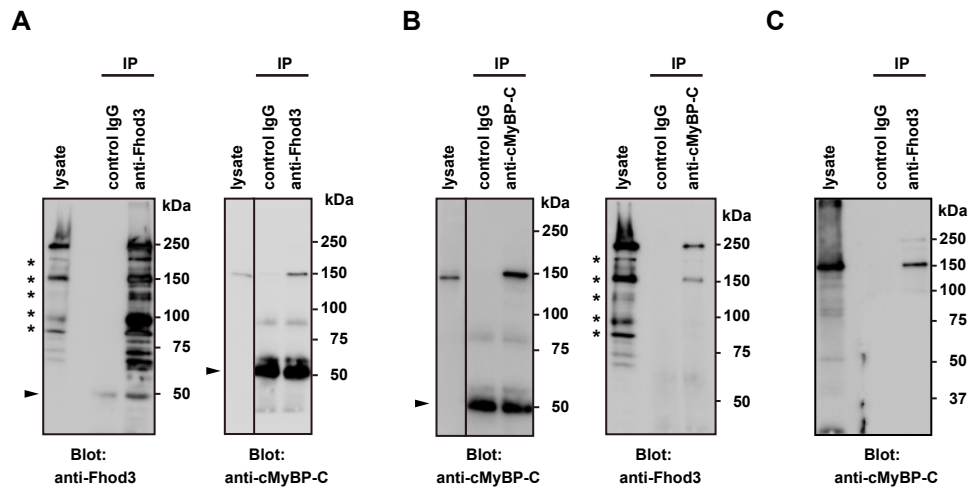


**Figure S5. Images of the uncropped immunoblots shown in Fig. 2, A, B, and C.** Asterisks and arrowheads indicate degradation products and immunoglobulins, respectively.

## Figure S6 (Matsuyama *et al.*)

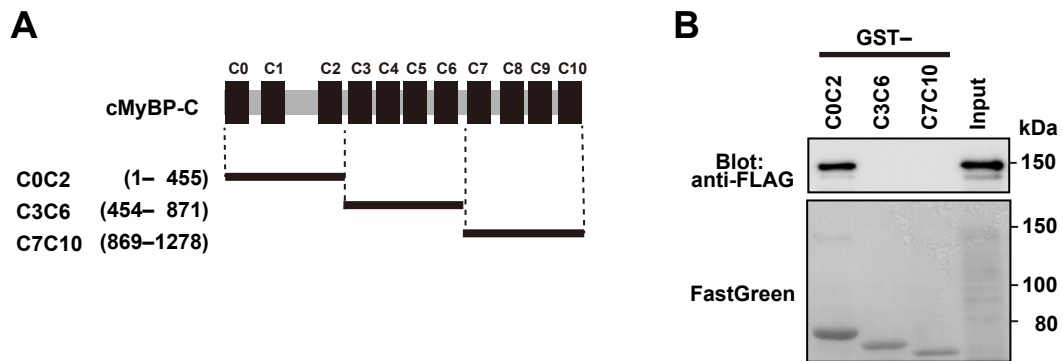


**Figure S6. Interaction of Fhod3 to the N-terminal region of cMyBP-C.** (A) Schematic structures of various cMyBP-C constructs used in (B). (B) The N-terminal region of Fhod3CM (Fhod3CM(N)) tagged with FLAG in the lysate of HEK-293F cells was incubated with indicated GST-fused fragments of cMyBP-C and pulled down with glutathione-Sepharose 4B beads. Precipitated proteins were subjected to SDS-PAGE and analyzed by immunoblot with the anti-FLAG antibody (upper panel) or stained with Fast Green. Positions for marker proteins are indicated in kDa.

**Figure S7 (Matsuyama *et al.*)**

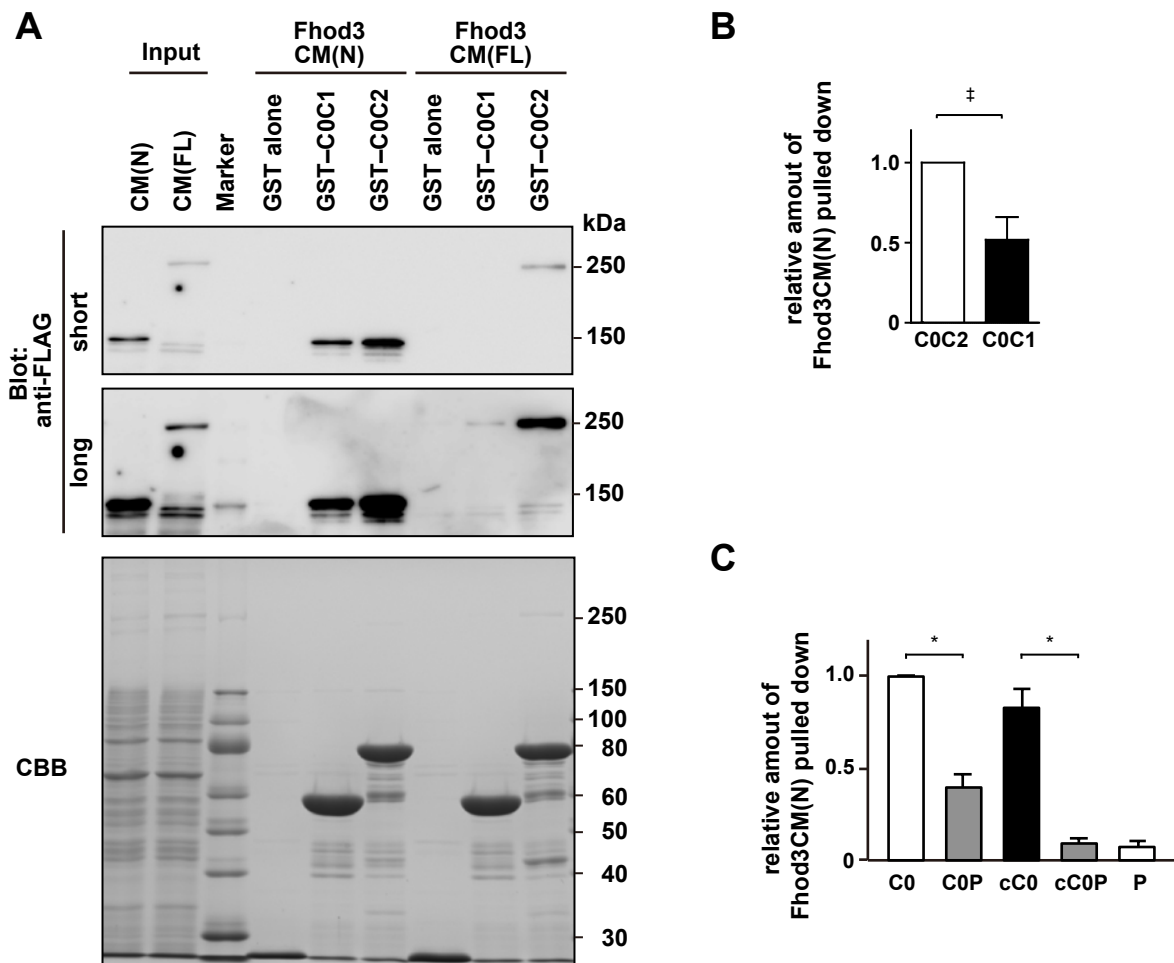


**Figure S7. Comparison of Fhod3-binding properties between C0C1 and C0C2.** (A) FLAG-tagged full-length (FL) or N-terminus (N) of Fhod3CM in the lysate of HEK-293F cells (input) was incubated with GST-cMyBP-C (C0C1 or C0C2) or GST alone and pulled down with glutathione-Sepharose 4B beads. Precipitated proteins were subjected to SDS-PAGE and analyzed by immunoblot with the anti-FLAG antibody (upper panel) or stained with CBB (lower panel). Positions for marker proteins are indicated in kDa. (B) Quantification of the band intensities of Fhod3CM(N) pulled down with C0C1 relative to those with C0C2 from seven independent pull-down experiments. Values are means  $\pm$  SD.  $\ddagger P < 0.05$ . (C) Quantification of the band intensities of Fhod3CM(N) pulled down with C0P, cC0, and cC0P relative to those with C0 from five independent pull-down experiments. Values are means  $\pm$  SD.  $*P < 0.001$ .

## Figure S8 (Matsuyama *et al.*)

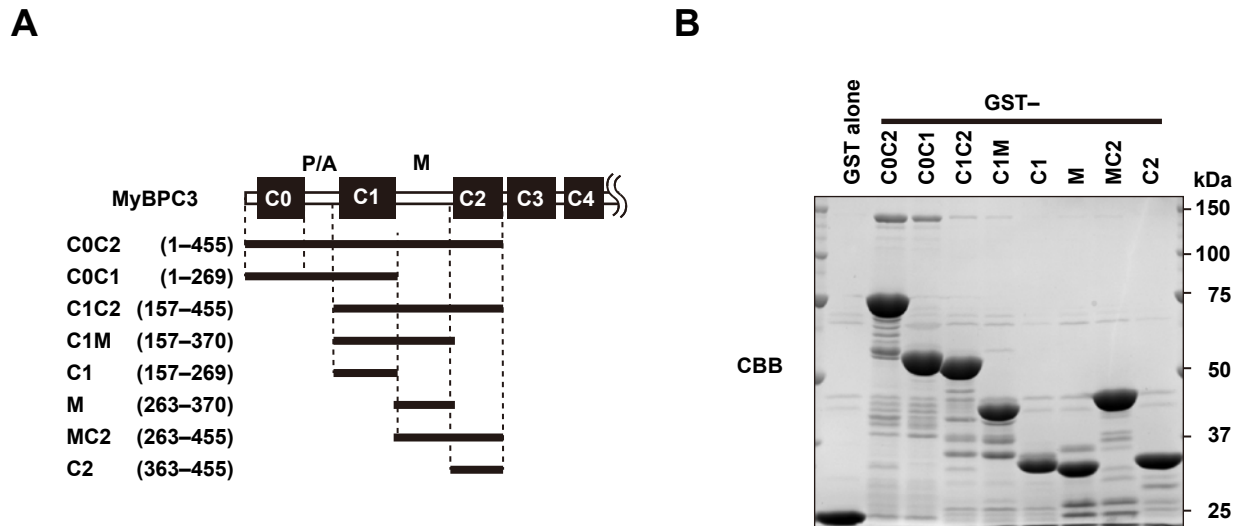


**Figure S8. Interaction of Fhod3 to cMyBP-C.** (A) Schematic structures of various cMyBP-C constructs used in (B). (B) The N-terminal region of Fhod3CM (Fhod3CM(N)) in the lysate of HEK-293F cells was incubated with indicated GST-fused fragments of cMyBP-C and pulled down with glutathione-Sepharose 4B beads. Precipitated proteins were subjected to SDS-PAGE and stained with CBB. Positions for marker proteins are indicated in kDa.

## Figure S9 (Matsuyama *et al.*)

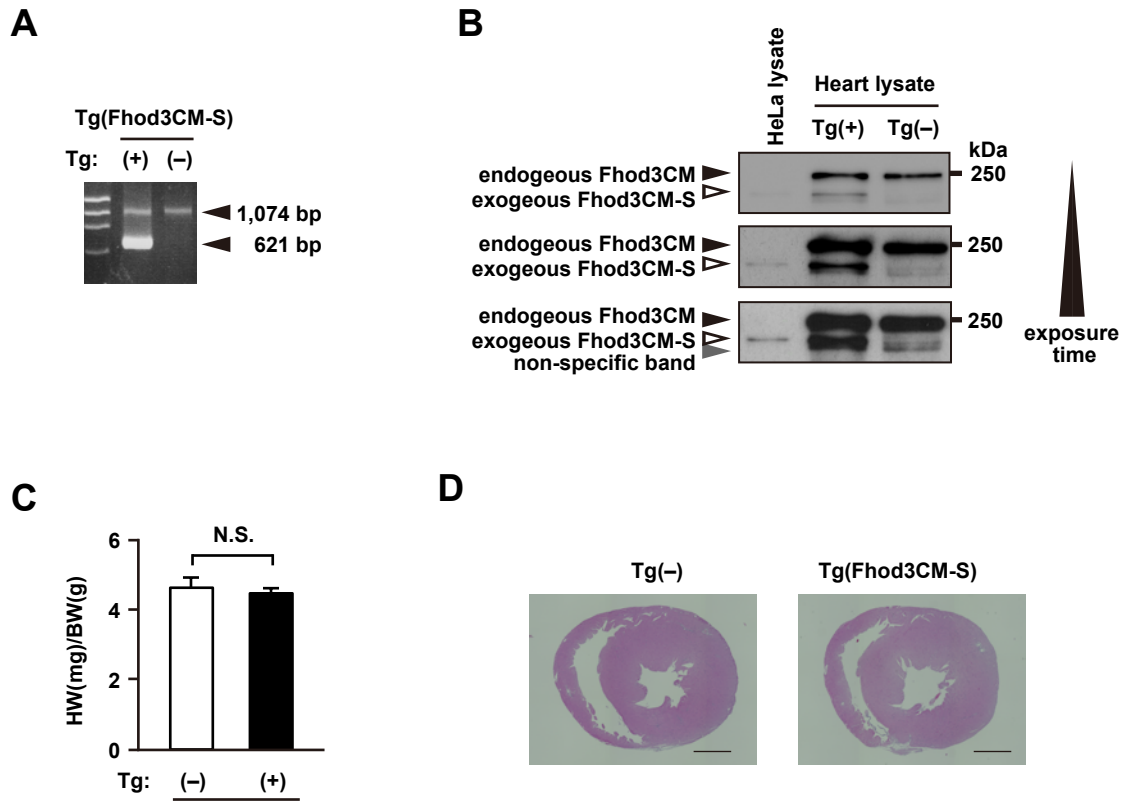


**Figure S9. Transgenic expression of Fhod3CM-S in the heart.** (A) RT-PCR analysis of the heart RNAs from transgenic Tg(Fhod3CM-S) (see Fig. 1E) or Tg(-) mice using a pair of primers located in exons 8 and 14 of Fhod3 (see Fig. 1E). The indicated bands of the lengths of 1,074 and 621 bp were the product from Fhod3CM and Fhod3CM-S, respectively. (B) Immunoblot analysis of Fhod3. Cardiac lysates from Tg(Fhod3CM-S) or Tg(-) mice and the lysate of HeLa cells expressing exogenous Fhod3CM-S were analyzed by immunoblot with the anti-Fhod3-(C-20). (C) Heart-to-body weight ratio of Tg(Fhod3CM-S) (n = 6) and Tg(-) (n = 6) mice at 24–36 weeks of age. Values are means (long bars)  $\pm$  SEM (short bars). N.S., not significant. (D) Histological analysis of hearts of Tg(Fhod3CM-S) and Tg(-) mice at 24–36 weeks of age. Short-axial sections of hearts were stained with hematoxylin and eosin. Scale bars: 1mm.

**Figure S10 (Matsuyama et al.)**

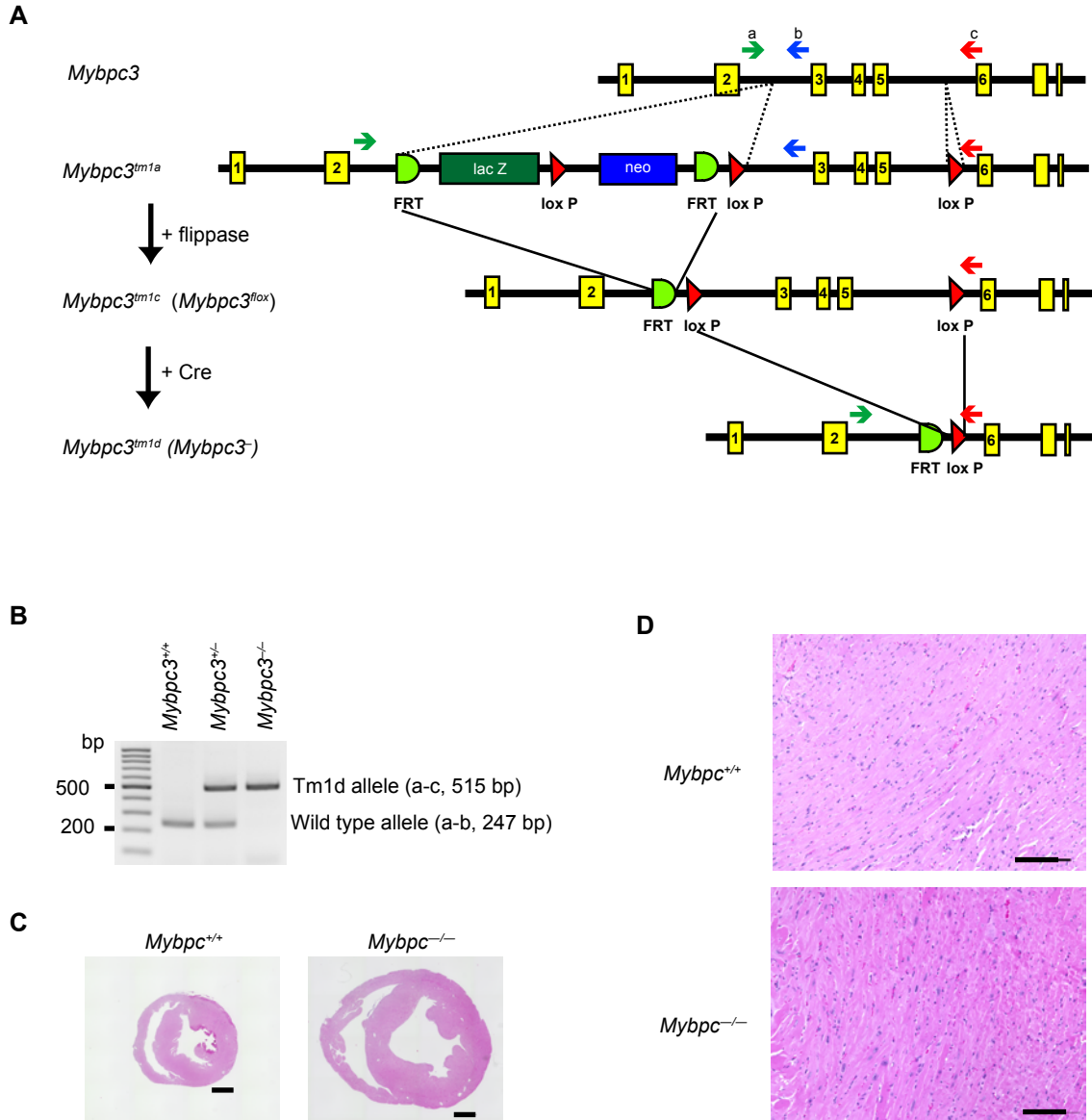


**Figure S10. Generation of cMyBP-C knockout mice.** (A) Schematic representation of the targeting strategy of knockout of cMyBP-C. Mice carrying the *Mybpc3<sup>tm1a</sup>* allele (EMMA ID EM:04690) were crossed with mice expressing flippase to obtain floxed *Mybpc3* allele (*Mybpc3<sup>fllox</sup>*). cMyBP-C knockout mice were generated by crossing the *Mybpc3<sup>fllox/+</sup>* with *Meox2<sup>Cre/+</sup>* mice, which express Cre recombinase in the embryo before implantation, and the offspring were further crossed with C57BL/6 to generate *Mybpc3<sup>+/-</sup>* mice without the Cre transgene. Small colored arrows indicate primers for PCR genotyping. (B) PCR analyses of tail DNA from *Mybpc3<sup>+/+</sup>*, *Mybpc3<sup>+/-</sup>*, and *Mybpc3<sup>-/-</sup>* mice. The PCR product from wild type allele was 247 bp in length, and the PCR product from null allele was 515 bp in length. (C and D) Histological analysis of hearts of cMyBP-C null mice (*Mybpc3<sup>-/-</sup>*) and control mice at 36 weeks of age. Short-axial sections of hearts (C) and short-axial-sectioned lateral wall of the left ventricles (D) were stained with hematoxylin and eosin. Scale bars: 1mm (C) and 100  $\mu$ m (D).

**Figure S11 (Matsuyama *et al.*)**

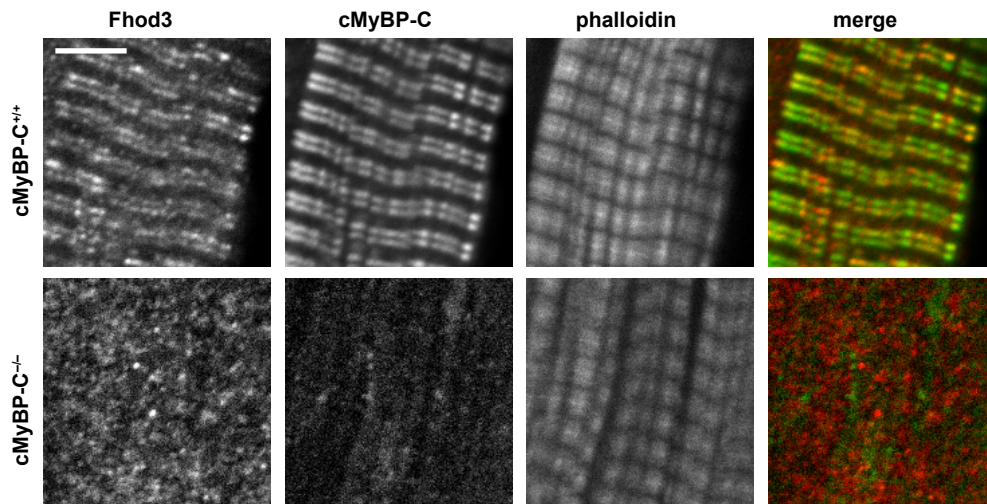


**Figure S11. cMyBP-C is required for Fhod3 localization to the C-zone.**

Sarcomeric localization of endogenous Fhod3 in the heart from cMyBP-C null mice. Sections of adult hearts from cMyBP-C null mice were subjected to immunofluorescent staining for Fhod3 (anti-Fhod3-(650-802); red) and cMyBP-C (green) followed by phalloidin staining (not depicted in merge). Scale bar, 5  $\mu$ m.

**Figure S12 (Matsuyama *et al.*)**

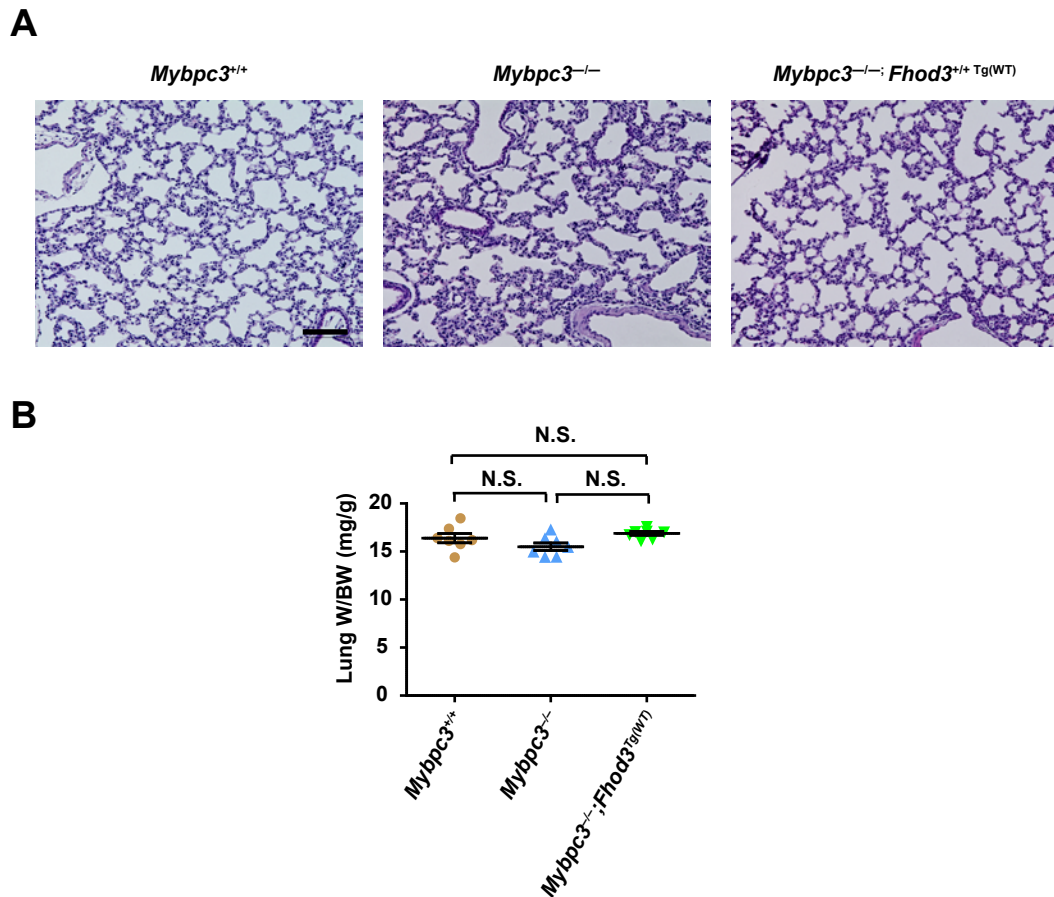


**Figure S12. Effects of transgenic overexpression of Fhod3 in cMyBP-C null mice on the lung.** (A) Histological analysis of lung of cMyBP-C null mice overexpressing Fhod3 (*Mybpc3<sup>-/-</sup>;Fhod3<sup>Tg(WT)</sup>*) and control mice (*Mybpc3<sup>+/+</sup>* and *Mybpc3<sup>-/-</sup>*) at P9. Sections of lung tissues were stained with hematoxylin and eosin. Scale bars, 100  $\mu$ m. (B) Lung-to-body weight ratio of cMyBP-C null mice overexpressing Fhod3 (*Mybpc3<sup>-/-</sup>;Fhod3<sup>Tg(WT)</sup>*, n = 7) and control mice (*Mybpc3<sup>+/+</sup>*, n = 7; *Mybpc3<sup>-/-</sup>*, n = 7) at P9. Values are means (long bars)  $\pm$  SEM (short bars). N.S., not significant.



**Figure S13 (Matsuyama et al.)**

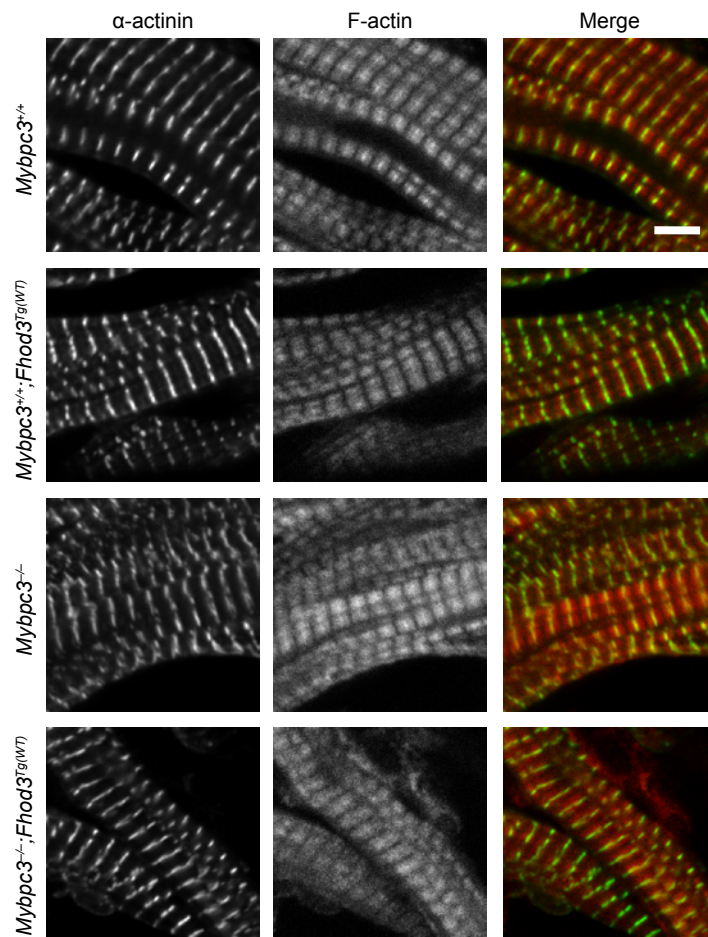


**Figure S13. Sarcomeric structures of hearts of cMyBP-C null mice overexpressing Fhod3 (*Mybpc3*<sup>-/-</sup>;*Fhod3*<sup>Tg(WT)</sup>) and control mice.** Sections of hearts from mice of the indicated genotypes were subjected to immunofluorescent staining for  $\alpha$ -actinin (green) and phalloidin (red). Scale bar, 5  $\mu$ m.

**Figure S14 (Matsuyama et al.)**

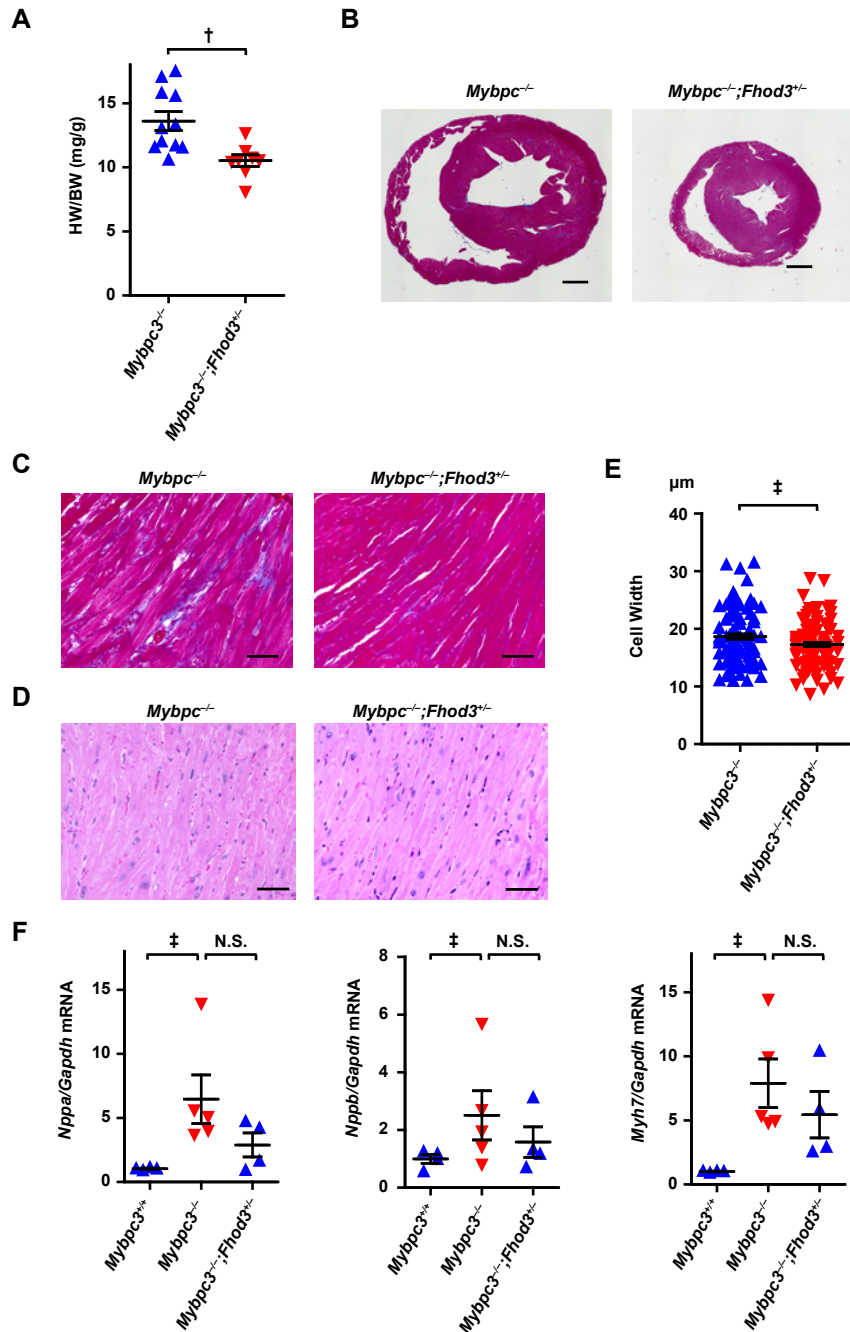


**Figure S14. Effect of heterozygous deletion of Fhod3 in cMyBP-C null mice at 36 weeks of age . (A)** Heart-to-body weight ratio of mice of the indicated genotypes (*Mybpc3*<sup>-/-</sup>, n = 11; *Mybpc3*<sup>-/-</sup>;*Fhod3*<sup>+/-</sup>, n = 8) at 36 weeks. Values are means (long bars) ± SEM (short bars). †P<0.01. (B–D) Histological analysis of hearts at 36 weeks. Short-axial sections of hearts (B) and short-axial-sectioned lateral wall of the left ventricles (C, D) were stained with azan (B, C) or hematoxylin and eosin (D). Scale bars: 1mm (B) and 50 μm (C, D). (E) The width of cardiomyocyte at the nuclei level by wheat germ agglutinin staining of left ventricle septum from mice of the indicated genotypes (*Mybpc3*<sup>-/-</sup>, n = 103; *Mybpc3*<sup>-/-</sup>;*Fhod3*<sup>+/-</sup>, n = 103) at 36 weeks was estimated by wheat germ agglutinin staining. Values are means (long bars) ± SEM (short bars). ‡P<0.05. (F) Quantitative real-time PCR analysis of fetal cardiac gene expression in mice with the indicated genotypes (*Mybpc3*<sup>+/+</sup>, n = 6; *Mybpc3*<sup>-/-</sup>, n = 7; *Mybpc3*<sup>-/-</sup>;*Fhod3*<sup>+/-</sup>, n = 6) at 36 weeks. Values are means (long bars) ± SEM (short bars). *Nppa*, encoding ANF; *Nppb*, encoding BNP; *Myh7*, encoding β-MHC; *Gapdh*, encoding GAPDH. ‡P<0.05; N.S., not significant.